Plume Budgets in Clear and Cloudy Convective Boundary Layers

ULRICH SCHUMANN

DLR, Institute of Atmospheric Physics, Oberpfaffenhofen, Germany

CHIN-HOH MOENG

National Center for Atmospheric Research, Boulder, Colorado

(Manuscript received 29 May 1990, in final form 25 February 1991)

ABSTRACT

From results of large-eddy simulations of the clear convective boundary layer and of a stratus-topped boundary layer, we evaluate the budgets of mass, momentum, heat, moisture, and turbulent kinetic energy within "plumes" that are formed by "updrafts" or "downdrafts." Each grid cell is classified as part of updrafts or downdrafts according to the sign of the resolved vertical velocity. By means of the divergence theorem and Leibniz' rule, the mixing flux across the interface between plumes can be computed from volume integrals. The general form of the budget equation is deduced and compared to previous two-stream models. Both the mean convective circulation and small-scale turbulent motions contribute to the mixing flux across the interface. The small-scale fluxes are largest near the inversion layer at the top of the boundary layers and are important also in the surface layers. Vertical and horizontal velocities in plumes are strongly influenced by the vertical mean pressure gradient and horizontal pressure forces at the plume's lateral surfaces. For the cloudy case, the plume budgets differ from those in the clear boundary layer because of latent heat release and radiation cooling near the cloud top. We find stronger downdrafts because of buoyancy and pressure forces. In both the clear and the cloudy cases, most of the kinetic energy of turbulence within the upper part of the downdrafts comes from the updrafts through lateral mixing, not from buoyancy forcing.

1. Introduction

Motions in the clear and the stratus-cloud-topped convective boundary layers are dominated by "plumes" of "updrafts" or "downdrafts" (Lenschow and Stephens 1980; Nicholls 1989). These plumes carry a large fraction of the vertical fluxes and justify, therefore, the "top-hat profile approximation," in which vertical fluxes are computed as if the vertical velocity and the transported quantity at a given height were horizontally constant within the plumes (Betts 1973). In a previous study (Schumann and Moeng 1991, hereafter referred to as SM) we used data from large-eddy simulation (LES) of convective boundary layers to compare various plume definitions. We found that the top-hat profile approximations give the most uniform approximation to the actual flux profiles and describe about 60% of the actual fluxes if the plumes are so-called w plumes. Such w plumes are classified according to the sign of vertical velocity w. Application of such approximations requires knowledge of the plume-averaged motion field. Here we continue the previous study (SM) and analyze the properties that determine the dynamics of w plumes.

Corresponding author address: Dr. Ulrich Schumann, DLR, Institut Für Physik der Atmosphäre, D-8031 Oberpfaffenhofen, Germany.

Models for the dynamics of plumes have been proposed by Telford (1970) on the concept of steadily rising thermals. Arakawa and Schubert (1974) set up a model for the ensemble of cumulus clouds relative to environmental air. Updraft and downdraft circulation models, based on the top-hat approximation and the assumption that both parts of the circulation have constant (in space and time) area fractions, have been deduced by Hanson (1981), Randall and Huffman (1982), and Wang and Albrecht (1986, 1990). Chatfield and Brost (1987) considered the budget of air components in updrafts and downdrafts, which they call "streams." These models require information on the plume geometry, the contributions from the resolved plume motions, and from the subplume turbulence; such data were presented in SM. Moreover, the models need data on the mixing between plumes, on the pressure forces driving the motions, and on the contributions to the budgets of the conserved quantities in such plumes. These data are difficult to deduce from measurements.

Few experimental studies have considered budgets of vertical velocity in updrafts and downdrafts using aircraft measurements at various heights within the boundary layer. Lenschow and Stephens (1980) deduced such a budget for updrafts in a clear convective boundary layer over the ocean. They use "q plumes"; that is, they classify updrafts as those parts of the mea-

sured flight legs where moisture fluctuations q' exceed a given threshold over a certain flight distance. Young (1988) analyzed data from a convective boundary layer over land and defined updrafts and downdrafts in terms of either positive or negative spatially filtered vertical velocity. He determined the budgets of vertical velocity for both updrafts and downdrafts. However, in both studies, the data were insufficient to separate the contributions from lateral mixing between updrafts and downdrafts and from pressure forces. Experimental data on plume budgets in convective boundary layers for quantities other than vertical velocity are not known to us.

In this paper we analyze results from the LES described in SM to determine the components of budgets for vertical and horizontal momentum, ρw and ρu; potential temperature θ or liquid water potential temperature θ_l; total moisture q (vapor plus liquid water); and turbulent kinetic energy E in updrafts and downdrafts. The turbulent kinetic energy is of interest because it is important for lateral entrainment between updrafts and downdrafts (Telford 1970) and for entrainment at the inversion above the mixed layer. Our conceptual model is similar to that of Chatfield and Brost (1987) and Young (1988). It approximates the vertical circulation from the ensemble of updrafts and downdrafts in convective boundary layers as two streams of variable cross section, one stream upward and the other downward. The ensembles are horizontally homogeneous but their properties are permitted to vary in the vertical. The theoretical concept would also apply to three classes of motions; for example, including environmental air between the updrafts and downdrafts. We determine the pressure forces and the mixing at the moving interface between the ensemble of updrafts or downdrafts and their respective environment. The related surface integrals are difficult to identify from gridpoint values. We will present a method to replace the surface integrals by volume integrals that can be approximated simply by sums over all grid points within a plume. The method is applied to determine the budgets for two types of boundary layers, the convective boundary layer (CBL) and the stratus-topped boundary layer (STBL) (details as given in SM). By this, we will see how latent heat release and radiation cooling at the cloud top change the plume properties relative to those in clear cases. Such information helps in understanding observed plume properties and forms the basis for testing plume models of clear and cloudy cases.

2. Analysis of plume budgets from LES

a. Conditional sampling method

As explained in SM, a time-dependent indicator function I_p is defined locally for a plume of type p, which discriminates between "updrafts" (subscript $p = u$) and "downdrafts" ($p = d$) (in principle more than two classes are conceivable). The indicator function is determined for each grid index i, j of the $M_x \cdot M_y$ grid cells in the computational domain at a given grid level z_k, $k = 1, \cdots, M_z$, or altitude z. In the present study, $I_u = 1$, if the local vertical velocity w is positive, otherwise $I_u = 0$. Similarly, $I_d = 1$ when $w \leqslant 0$, and $I_d = 0$ elsewhere. The computational domain covers the horizontal area $A = M_x M_y \Delta x \Delta y$. The horizontal cross section taken by the plumes within the computational domain at height z_k is $A_p = \Delta x \Delta y \sum_{i=1}^{M_x} \sum_{j=1}^{M_y} I_p(i, j, k)$. The fractional area of the plumes at height z_k equals $\alpha_p = A_p/A$.

Mean values of any function f in the computational domain at height z_k are defined, in the notation of Young (1988), discretely by

$$[f]_p(z_k) = \sum_{i=1}^{M_x} \sum_{j=1}^{M_y} I_p(i, j, k) f(i, j, k) / \sum_{i=1}^{M_x} \sum_{j=1}^{M_y} I_p(i, j, k), \quad (1)$$

but may also be understood in the continuous sense for infinitesimal grid spacings as

$$[f]_p(z) \approx \frac{1}{\Delta V_p} \iint_{\Delta V_p} \int f(x, y, z) dV \approx \frac{1}{A_p} \int_{A_p} \int f(x, y, z) dS, \quad (2)$$

whatever gives the more convenient notation. As sketched in Fig. 1, the volume ΔV_p consists of a horizontal slice of thickness Δz in height with cross-section area A_p, $\Delta V_p = A_p \Delta z$. Note that this slice horizontalwise consists, in general, of several nonconnected slices of the various plumes of given type p inside the computational domain. The plume mean value $[f]_p$ differs from the horizontal (or ensemble) mean value $\bar{f}$, which averages over all plumes:

$$\bar{f} = \sum_p \alpha_p [f]_p. \quad (3)$$

To simplify notation, we omit the brackets where possible without ambiguity and introduce deviations f''_p from the plume's mean value, whereas the conventional fluctuations around the ensemble mean are denoted by f':

$$f''_p = f - f_p, \quad f' = f - \bar{f}. \quad (4)$$

We also define the plume-surface mean value, which averages over the lateral surface ΔS_p of a plume slice of thickness Δz, see Fig. 1:

$$[f]_{S_p} = \frac{1}{\Delta S_p} \int \int_{\Delta S_p} f dS. \quad (5)$$

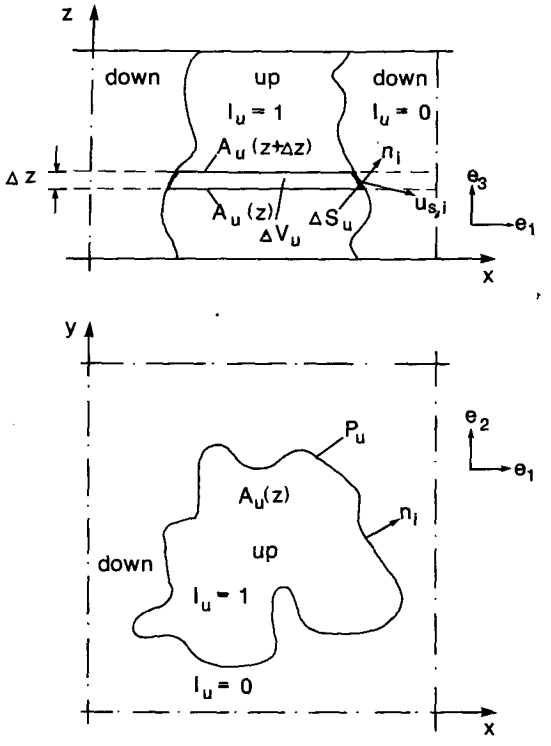

FIG. 1. Sketch of the plume geometry. I_u: indicator function for updrafts, Δz: slice thickness, ΔV_u: updraft volume at level z, A_u: cross section, P_u: perimeter, $\{n_i\}$: plume-surface normal vector, $\{e_i\}$: unit coordinates; $\{u_i\}$: fluid velocity; $\{u_{S,i}\}$: plume-surface velocity.

b. *Leibniz' rule and divergence theorem*

For later usage, we refer to Leibniz' rule

$$\iint_{\Delta V_p} \int \frac{\partial f}{\partial t}\, dV = \frac{\partial}{\partial t} \iint_{\Delta V_p} \int f dV - \iint_{\Delta S_p} n_i u_{s,i} f dS, \quad (6)$$

where n_i is the outer unit vector normal to the surface of the volume ΔV_p, and $u_{S,i}$ is the vector of the velocity of this surface. The summation convention is used everywhere for repeated lower indices. Note that $u_{s,i}$ differs from the fluid velocity u_i. The upper and lower plane surface bounding the slice of thickness Δz are fixed in space and, therefore, the surface velocity $u_{s,i}$ is identical to zero on these parts of the volume's surface. For this reason, the given surface integral is taken over the lateral surface only. If one divides the above equation by ΔV_p and employs the previous definitions of plume mean values, one obtains

$$\left[\frac{\partial f}{\partial t}\right]_p = \frac{\partial}{\partial t}[f]_p - D_p^{-1}[n_i u_{s,i} f]_{S_p}, \quad (7)$$

where $D_p = \Delta V_p / \Delta S_p$. The length scale will not be computed explicitly. It equals one-fourth of the diameter of an equivalent circular plume [as introduced by Lenschow and Stephens (1980)] if the plume boundaries are vertical but is smaller otherwise.

Likewise, we express the divergence theorem (with $w = u_3$):

$$\iint_{\Delta V_p} \int \frac{\partial}{\partial x_i}(u_i f) dV = \iint_{A_p(z+\Delta z)} w f dS - \iint_{A_p(z)} w f dS + \iint_{\Delta S_p} n_i u_i f dS, \quad (8)$$

for $\Delta z \to 0$, as

$$\left[\frac{\partial}{\partial x_i}(u_i f)\right]_p = \alpha_p^{-1} \frac{\partial}{\partial z}(\alpha_p [w f]_p) + D_p^{-1}[n_i u_i f]_{S_p}. \quad (9)$$

These relationships will be used in the subsequent section.

c. *General form of the plume budgets*

The objective of this section is to deduce the budget equations for plumes in a form such that its terms can be evaluated from the LES result. The problem here is that the budget will contain surface integrals which are difficult to identify from gridpoint values. Thus, we seek to replace the surface integrals by volume integrals that can be approximated simply by sums over all grid points within a plume.

The derivation of the budget equation for the plume mean value of any quantity f starts from the instantaneous local equation for f, to which we apply the averaging operator $[\ ]_p$ term by term:

$$\left[\frac{\partial f}{\partial t}\right]_p + \left[\frac{\partial}{\partial x_i}(u_i f)\right]_p = [Q_f]_p. \quad (10)$$

The source terms Q_f are specified in the Appendix for various fields f, but the analysis of the mixing between plumes will be performed without knowing the sources explicitly. Using Eqs. (7) and (9), Eq. (10) is converted into

$$\frac{\partial}{\partial t}[f]_p + \alpha_p^{-1} \frac{\partial}{\partial z}(\alpha_p [w f]_p) + D_p^{-1}[n_i (u_i - u_{s,i}) f]_{S_p} = [Q_f]_p. \quad (11)$$

For $f = 1$ or for $f = \rho = \text{const.}$, we have the continuity equation

$$\alpha_p^{-1} \frac{\partial}{\partial z}(\alpha_p [w]_p) + D_p^{-1}[n_i (u_i - u_{s,i})]_{S_p} = 0, \quad (12)$$

where the first term describes the vertical divergence of the mass flux at a given height within the plume, and the second the net mass flux across the plume's lateral surface at the same height.

Now we split the function f into its horizontal (ensemble) mean value $\bar{f}$ and its fluctuating part $f' = f - \bar{f}$ and insert this into Eq. (11). Moreover, we use (12) to simplify terms including the mean field $\bar{f}$ and obtain

$$\frac{\partial}{\partial t}[f]_p + \alpha_p^{-1}\frac{\partial}{\partial z}(\alpha_p[w'f']_p) + M_{f,p} + [w]_p\frac{\partial \bar{f}}{\partial z} = [Q_f]_p. \quad (13)$$

Here the "mixing term"

$$M_{f,p} = D_p^{-1}[n_i(u_i - u_{s,i})f']_{S_p} \quad (14)$$

represents transport of the conserved quantity across the interface between plumes. It defines the mixing at the plume's lateral surface due to entrainment and detrainment between a plume and its environment. It describes the net effect; i.e., $M_{f,p}$ is zero if the amount of f that is entrained equals the amount that is detrained. Hence, $M_{f,p}$ is zero if f = const, so that $f' = 0$, although the amount of fluid exchange might be considerable. All the other terms in Eq. (13) describe solely internal transports within the plume and external sources.

For given source terms Q_f, one could evaluate the mixing term $M_{f,p}$ as the residual from Eq. (13). Since the source term may be difficult to reevaluate by analysis from given LES results and even more difficult from measurements, an alternative method is described below. For this purpose, we perform the difference of Eq. (10) (with $f = \bar{f} + f'$) and (13) and obtain, using local continuity ($\partial u_i/\partial x_i = 0$),

$$M_{f,p} = \left[\frac{\partial}{\partial x_i}(u_i'f')\right]_p + \left[\frac{\partial f}{\partial t}\right]_p - \frac{\partial}{\partial t}[f]_p - \alpha_p^{-1}\frac{\partial}{\partial z}(\alpha_p[wf']_p). \quad (15)$$

From this equation we can evaluate the mixing between a plume and its environment without having to know the surface details. It can easily be evaluated from the LES where all the local fields and the local time derivatives are available.

In order to identify the contributions that are resolvable by a plume model as far as possible, we follow Young (1988) and split the vertical fluxes contained in Eq. (13) into fluxes from plume mean values according to the top-hat approximation and subplume contributions:

$$[w'f']_p = w_p([f]_p - \bar{f}) + [w_p''f_p'']_p. \quad (16)$$

With this splitting, Eq. (13) (omitting brackets where possible) forms the basis for the discussion of the numerical results, as

$$\frac{\partial}{\partial t}f_p = -\alpha_p^{-1}\frac{\partial}{\partial z}(\alpha_p w_p(f_p - \bar{f})) - \alpha_p^{-1} \times \frac{\partial}{\partial z}(\alpha_p[w_p''f_p'']_p) - w_p\frac{\partial \bar{f}}{\partial z} + Q_{f,p} - M_{f,p}. \quad (17)$$

Here the first term on the rhs describes contributions to f from mean vertical advection within plumes, the second gives the contributions from vertical subplume mixing, the third describes advection by vertical plume motion times the ensemble mean gradient of the conserved field, the fourth contains the additional sources within the plume, and the last contains the mixing loss. If one multiplies with α_p and sums over all classes of plumes p, according to Eq. (3), one obtains the budget of the horizontal mean field $\bar{f}$. The effect of interplume mixing is zero in this sum:

$$\sum_p \alpha_p M_{f,p} = 0. \quad (18)$$

Equation (17) forms the general basis for plume modeling.

d. Discussion and comparison to previous proposals

The budget equation for vertical velocity (with zero mean value $\bar{w}$) can be deduced from Eq. (17) and the source term as given in Eq. (31) of the Appendix is

$$\frac{\partial}{\partial t}w_u = -\alpha_u^{-1}\frac{\partial}{\partial z}(\alpha_u(w_u)^2) - \alpha_u^{-1}\frac{\partial}{\partial z}(\alpha_u[w_u''^2]_u) - \rho^{-1}\frac{\partial \bar{p}}{\partial z} + [\beta g\theta_v']_u - [\rho^{-1}\partial p'/\partial z]_u - M_{w,u}, \quad (19)$$

where

$$M_{w,p} = D_p^{-1}[n_i(u_i - u_{s,i})w']_{S_p} \quad (20)$$

describes the net loss of vertical momentum from plumes by mixing across the plume's lateral surface. The mixing term would be identical to zero if we were using w plumes in the strict sense of zero vertical velocity at the interface between plumes because the transported quantity w' would be zero at that surface. (This does not mean that mixing terms $M_{f,p}$ are small for other transported quantities f with nonzero fluctuations at the plume's surface.) In practical measurements or numerical simulations this strict definition cannot be implemented, and, therefore, there will always be mixing at least on the subgrid-scale level. However, the mixing of vertical momentum should be definitely smaller for w plumes than for either q plumes or wq plumes (SM) or any other plume definition. For this reason, the mixing term discussed by Young (1988) should be small, because his definition of plumes is based on low-pass-filtered vertical velocity with a cutoff wavelength of $0.1z_i$. His approach is actually very sim-

ilar to our procedure of using grid-filtered variables to identify the plumes.

The vertical acceleration of mean plume vertical motion, $\partial[w]_p/\partial t$, is zero in steady state. In reality, the convective circulation will take some time to approach this steady state even for fixed values of the surface heat flux and the boundary-layer depth. Young (1988) accounted only for changes induced by the latter by including the time derivative of the normalization velocity w_* into the budget. However, in general, the acceleration $\partial[w]_p/\partial t$ is small in comparison to other terms in Eq. (19). Moreover, the sum of the local accelerations, weighted with their fractional area α_p, over updrafts, downdrafts, and possibly environmental air—see Eq. (3)—is identically zero because of continuity and $\bar{w} = \sum_p \alpha_p w_p = 0$, except for mean subsidence changes. This sum relates the mean pressure gradient to the vertical velocity variance,

$$-\partial\bar{p}/\partial z = \partial(\rho\overline{w^2})/\partial z. \tag{21}$$

Obviously, the mean pressure gradient balances a large fraction of the vertical advection terms in Eq. (19).

For the q plumes considered by Lenschow and Stephens (1980), the vertical velocity fluctuations are nonzero at the interfaces between a plume and its environment. As a consequence, the mixing term $M_{w,p}$, which Lenschow and Stephens called the edge-effect $E_{w,p}$, should have a significant magnitude. They determined $E_{w,p} - [\partial p/\partial z]_p$ as the residual of their budget equation. Because of unknown pressure effects, they were not able to differentiate between mixing and pressure forcing. Moreover, comparing the result of Lenschow and Stephens [1980, their Eq. (16)], with the present result as given in Eq. (17), we find that their edge-effect term, $E_{w,p}$, is related to our mixing term by

$$E_{w,p} = M_{w,p} + w_p\left(\alpha_p^{-1}\frac{\partial}{\partial z}(\alpha_p w_p)\right) + [w_p''^2]_p\left(\alpha_p^{-1}\frac{\partial\alpha_p}{\partial z} - d_p^{-1}\frac{\partial d_p}{\partial z}\right). \tag{22}$$

The profile of the plume diameter d_p differs from that of the area fraction α_p (see SM), so that the last term is nonzero. We see that part of the edge effect can be computed from plume mean values.

3. Results and discussions

In this section, the budget components will be presented and discussed as computed from the LES. In the discussions we refer to the previous paper (SM) where we have presented plume-mean values. The sign of the plotted budget components is selected such that positive terms, according to Eq. (17), increase the quantity under consideration. In most figures, the results are normalized by the depth of the boundary layer, z_i, and the convective scales w_*, T_*, which are defined as usual (SM). We will find that some of the results show considerable oscillations. These oscillations are particularly large for quantities computed from finite differences of mean profiles. Similar effects have been found by Moeng and Wyngaard (1989) for the dissipation rate which was computed, from the same data, as the residual of the energy budget. These oscillations are to be considered as spurious results of insufficient data for computing the ensemble average or are effects of finite-difference approximation errors.

a. The mass fluxes and pressure in and between plumes

According to the continuity equation (12), the mean vertical divergence within an updraft and the mixing from downdrafts into updrafts has been evaluated, see Fig. 2. Both terms represent contributions to the specific volume balance within an updraft. The mixing term

$$M_u = D_u^{-1}[n_i(u_i - u_{s,i})]_{S_u} = -\alpha_u^{-1}\frac{\partial}{\partial z}[\alpha_u w_u]_u \tag{23}$$

is nonzero because of the vertically changing area fraction and mean velocity in updrafts (see SM). The mixing term describes the net outflux from the updrafts into downdrafts, both due to the mean convective circulation and the small-scale turbulent mixing. The zero value of M_u in the middle of the mixed layer means that the net mass exchange between updrafts and downdrafts is zero there; it does not mean that mixing is zero at this level. As to be expected from the general circulation pattern, $-M_u$ is positive in the lower part of the mixed layer and negative above. At the inversion, the sign of M_u oscillates, which may be spurious as explained before. The mixing term is balanced exactly, for continuity, by the divergence of the vertical mean volume flux. In the present normalization, Fig. 2 shows that the mixing is only a little larger in STBL than in the CBL. The additional buoyancy induced by radiation cooling at the cloud top and the latent heat release

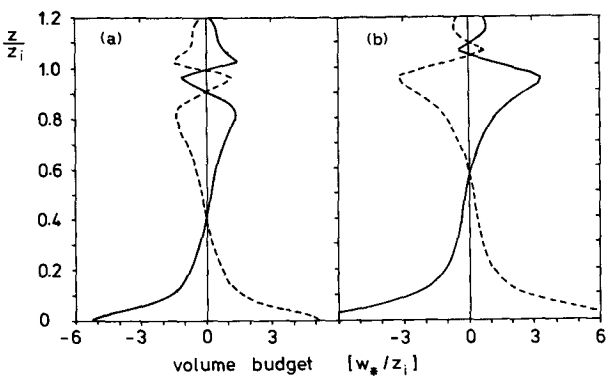

FIG. 2. Contributions to continuity equation (volume budget) in (a) the CBL and (b) the STBL. The line coding corresponds to the individual terms in $-\alpha_u^{-1}\partial(\alpha_u[w]_u)/\partial z - M_u = 0$ as solid (first term) and dashed (second term).

in the cloudy updrafts increase the circulation intensity, in particular near the inversion, but also at the bottom surface.

The pressure field is a function of the vertical accelerations in the plumes and the horizontal accelerations of the convective circulation between updrafts and downdrafts. No model exists, yet that predicts these properties in detail. For example, Telford (1970) had to assume that the pressure profiles are the same in updrafts and downdrafts with no horizontal pressure differences between the plumes. Therefore, it is of interest to see the LES results for the plume-averaged pressure profiles in updrafts and downdrafts, both for CBL and STBL, as shown in Fig. 3. The ensemble mean of the pressure profile, i.e., $\alpha_u p_u + \alpha_d p_d = \bar{p}(z)$, equals the negative ensemble mean profile of vertical velocity variance, see Eq. (21). The difference in pressure between updrafts and downdrafts induces the horizontal parts of the convective circulation. This pressure difference is negative in the surface layer and positive near the inversion, see Fig. 3. This difference is, however, not a simple function of the vertical velocity, as can be seen from the fact that the pressure differences between updrafts and downdrafts vanishes at an altitude that differs from the altitude where the mixing flux M_u gets zero. The pressure difference is larger in the STBL than in the CBL. This is caused by the more vigorous circulation, as can be seen from the larger mass-flux budgets in Fig. 2, and also by differences in the horizontal scales of updrafts and downdrafts. We found larger normalized horizontal scales in the LES results for the STBL than for the CBL (SM).

b. *Budgets in the CBL*

Figure 4 depicts the individual terms contributing to the budget of vertical momentum in the ensemble of updrafts of the CBL, i.e., the six terms on the rhs of Eq. (19) for $p = u$. The sum of all terms represents the mean tendency $\partial w_u/\partial t$ of vertical motion. Its magnitude is of order $0.5 w_*^2/z_i$. It is not exactly zero because the circulation intensity increases with the slowly growing boundary layer height and because we are averaging over a finite set of data in which the actual mean values still deviate from the ensemble mean value. We see from Fig. 4b (dotted curve) that the mixing term is small and typically of the same magnitude as the remaining vertical acceleration. As noted before, it would be zero exactly if subgrid-scale contributions to fluxes were neglected because the resolved vertical velocity is zero at the interface between updrafts and downdrafts. The mixing source $-M_{w,u} = D_u^{-1} \times [n_i u_{s,i} w']_{S_u} - D_u^{-1}[n_i u_i w']_{S_u}$ is positive. This is surprising because it requires some countergradient flux for which we have no clear physical explanation. It is positive presumably because the first term in the above sum dominates; the plume's surface normal velocity $n_i u_{s,i}$ contains the component $n_3 w_s$, which may be nonzero even at the resolved scales so that a positive correlation with w' appears possible. If the same LES results are analyzed using T plumes instead of w plumes (i.e., a plume definition based on the sign of temperature fluctuations), $-M_{w,u} z_i w_*^{-2}$ reaches a maximum of 1.2 near $z/z_i = 0.2$ but a strongly negative minimum of -5 at the inversion. This large sensitivity to the type of plume definition is consistent with our interpretation.

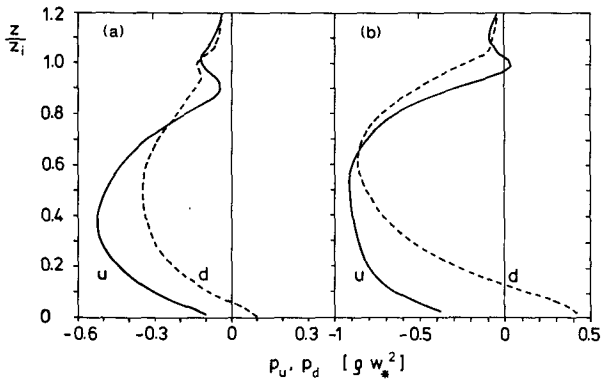

FIG. 3. Vertical pressure profiles in updrafts (full curves) and downdrafts (dashed curves), for (a) the CBL and (b) the STBL.

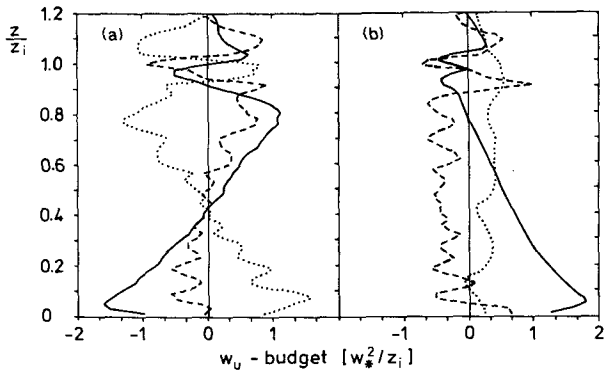

FIG. 4. Contributions to the budget of vertical velocity in updrafts of the CBL, $\partial w_u/\partial t$ = (a) $-\alpha_u^{-1}\partial(\alpha_u(w_u)^2)/\partial z - \alpha_u^{-1}\partial(\alpha_u[w_u''^2]_u)/\partial z - \rho^{-1}\partial\bar{p}/\partial z$ and (b) $[\beta g\theta_v']_u - [\rho^{-1}\partial p'/\partial z]_u - M_{w,u}$. In (a) and (b) the solid, dashed, and dotted lines correspond to the respective terms.

The updraft circulation is driven mainly by buoyancy; full curve in part (b) of Fig. 4. The small negative contributions at the inversion are either due to overshooting thermals or result from small-scale circulations at the inversion. The mean vertical advection, the first term [full curve in (a)], transports vertical momentum generated in the lower part of the mixed layer upward into the upper part of the mixed layer, where buoyancy is weaker. Small-scale plume turbulence [dashed curved in (a)] supports the mean advection but at a smaller rate.

Both the ensemble-mean pressure profile $\bar{p}$ and the

local fluctuations p' around this mean contribute to vertical accelerations. The plume-averaged pressure profiles p_u and p_d have been shown in Fig. 3. The mean vertical pressure gradient contributes strongly to vertical motions, see the dotted curve in Fig. 4a. It accelerates upward motion in the lower half and decelerates it in the upper half. The upward acceleration from the mean vertical pressure gradient within the lower half of the updrafts has also been noted by Lenschow and Stephens (1980). However, their profile assumption, $-[\partial p/\partial z]_u z_i(\rho w_*^2)^{-1} > 0.9(z/z_i)^{-1/3}$, is not supported by our result, which shows a more linear trend of the pressure gradient with height. In contrast to the mean pressure, the small-scale pressure fluctuations (dashed curve in Fig. 4b) contribute relatively little to the budget. The pressure gradient term $[\partial p'/\partial z]_u$ equals $\alpha_u^{-1}\partial/\partial z(\alpha_u[p']_u) - D_u^{-1}[n_3 e_3 p']_S$, where $n_3 e_3$ defines the projection of the surface normal into the vertical direction. In the present simulations, it has been found that the surface contribution is negligibly small. This fact may be useful for model simplifications. In hydrostatic flows, the pressure gradient should just balance the buoyancy forces. The dynamics of updrafts obviously depart strongly from hydrostatic behavior because of large advective accelerations. This is different in the lower part of downdrafts (not plotted) where pressure forces balance the buoyancy forcing to a larger extent; i.e., the flow in downdrafts is more hydrostatic than in updrafts. However, in the upper part of the boundary layer, where buoyancy is still positive or small, the sinking motions are driven by the plume-averaged vertical gradient of the mean and fluctuating pressure. This corroborates Young's (1988) conjecture that the pressure forcing provides the initial impetus to CBL downdrafts.

The budget for the x component of the horizontal velocity u in updrafts is presented in Fig. 5. A similar result can be computed for the y component (not plotted). We recall (see SM) that the downstream velocity $\bar{u}$ is of order 10 m s^{-1}. The vertical gradient $d\bar{u}/dz$ of the horizontally averaged upstream velocity $\bar{u}$ is small in the mixed layer but large near the bottom surface and in the inversion layer. Updrafts have a smaller downstream velocity u_u than downdrafts because the fluid in the updraft has experienced the surface friction and is, therefore, more retarded than the fluid in the downdrafts which still carry the stronger momentum from above the boundary layer. In Fig. 5, the individual terms of the budget are plotted according to Eq. (17) for $f = u$ (see the figure legend). The sum (not plotted) of the five components shown specifies the mean acceleration of the horizontal velocity within updrafts. It is negative near the bottom surface ($-w_*^2/z_i$) and near the inversion ($-1.5\ w_*^2/z_i$) and slightly negative but small in the remainder of the layer. The retardation at the lower surface is due to friction. The retardation at the inversion reflects the downward momentum transport within the boundary layer. Subplume motions are

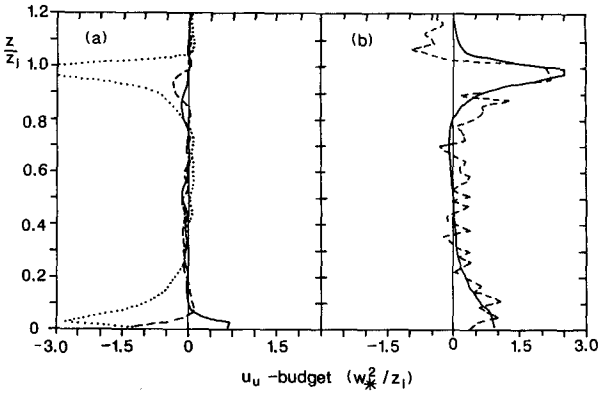

FIG. 5. Contributions to the budget of horizontal velocity in updrafts of the CBL, $\partial u_u/\partial t$ = (a) $-\alpha_u^{-1}\partial(\alpha_u w_u(u_u - \bar{u}))/\partial z - \alpha_u^{-1}\partial(\alpha_u[w_u'' u_u'']_u)/\partial z - w_u\partial\bar{u}/\partial z$ and (b) $-[\rho^{-1}\partial p'/\partial x]_u - M_{u,u}$. The lines correspond to terms as in Fig. 4 in (a) or Fig. 2 in (b).

important in the shear layer near the lower surface. They transfer the downward momentum flux from plume scales to the surface, and this causes the resultant flux divergence as given by the dashed curve in Fig. 5a. Above the surface layer, small-scale fluxes have negligible divergence. Mean vertical motions in the updrafts transport slow fluid upwards and, hence, $-w_u\partial\bar{u}/\partial z$ forms the main source for decelerating the updraft's velocity in the surface layer and even more at the inversion, see the dotted curve in (a). The convergence and divergence between the faster moving downdrafts and the slower updrafts induce a pressure field that tends to reduce the difference in plume velocities in x direction, in particular in the surface layer and near the inversion. The related mean horizontal pressure gradient, full curve in (b), is consistent with the estimate

$$[\partial p/\partial x]_u \sim \alpha_u^{-1}\rho(w_u - w_d)\partial\bar{u}/\partial z, \qquad (24)$$

which follows from the linear theory given by Rotunno and Klemp (1982) for pressure fluctuations induced by updrafts (and downdrafts) in a unidirectionally sheared environment. The factor α_u^{-1} is included because the mean horizontal gradient of pressure fluctuations is zero in the ensemble mean given by Eq. (3). Also, the mixing term [dashed curve in (b)] contributes positively to horizontal acceleration because the fluid mixed in from downdrafts into updrafts has larger horizontal speed. The magnitude of this mixing effect is about the same as that from the horizontal pressure gradient; i.e., large-scale dynamics and small-scale mixing are of comparable importance.

The budget for the horizontal velocity in downdrafts (not plotted) shows the same general trends as the updrafts except for reversed signs. The mixing sink in the updrafts equals the mixing source in the downdrafts up to factors α_p, see Eq. (18). The first two terms from the updraft and downdraft budgets (multiplied by the

respective area fractions) equal the horizontally averaged divergence of the vertical flux of horizontal momentum $\overline{u'w'}$, which is shown in SM.

The profile of the temperature deviation $\theta'(z)$ from ensemble mean $\bar{\theta}(z)$ corresponds to the buoyancy term in Fig. 4b. In Fig. 6, we show the budget of potential temperature in the updrafts. The updraft is heated from the bottom surface by small-scale turbulence, and the corresponding flux divergence is depicted by the dashed curve. The heat from this source is distributed across the mixed layer by advection of temperature differences, the full curve. Additional heating occurs in the lower part of the mixed layer due to upward advection against the decreasing mean temperature gradient (the dotted curve). Above the height of the temperature minimum ($z \approx 0.3z_i$) this term is converted into the most important cooling term. This vertical advection effect is balanced by the mixing of cooler air from downdrafts into the updrafts in the lower half [see full curve in (b)] and reverse in the upper half of the boundary layer. The sum (not plotted) of the four terms shown represents the mean temperature change in the updrafts. Because of surface heating, it is of order unity in the convective units throughout the mixed layer; it is slightly negative at the inversion because of the increasing boundary layer height. The downdraft budget of temperature shows trends similar to those in updrafts with reversed signs, except for the first two terms; the weighted sum of these two terms from both updraft and downdraft budgets equals the mean divergence of vertical temperature flux. This sum amounts to about $w_* T_* / (0.8 z_i)$ in the mixed layer, where $0.8z_i$ corresponds to the height where the total vertical heat flux $\overline{w'\theta'}$ becomes zero, see SM.

Figure 7 depicts the seven terms contributing to the updraft budget of kinetic energy $E = u_i'^2/2$, of turbulent motions in the updrafts. Vertical buoyancy flux,

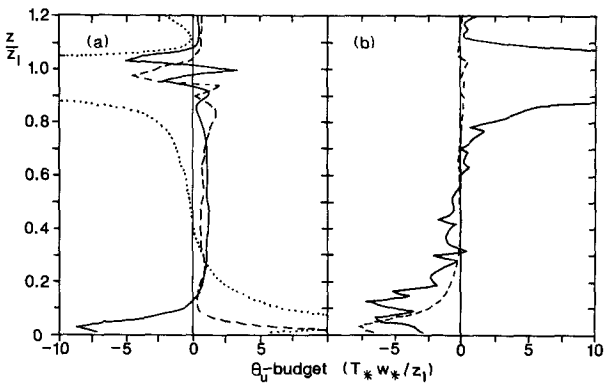

FIG. 6. Contributions to the budget of potential temperature in updrafts of the CBL, $\partial\theta_u/\partial t$ = (a) $-\alpha_u^{-1}\partial(\alpha_u w_u(\theta_u - \bar{\theta}))/\partial z - \alpha_u^{-1}\partial(\alpha_u[w_u''\theta_u'']_u)/\partial z - w_u\partial\bar{\theta}/\partial z$ and (b) $-M_{\theta,u}$. Lines correspond to terms as in preceding figures. The dotted curved in (a) and the full curve in (b) reach extreme values of about ±200 near the inversion. The dashed curve in (b) represents the model result, Eq. (25), for the mixing term.

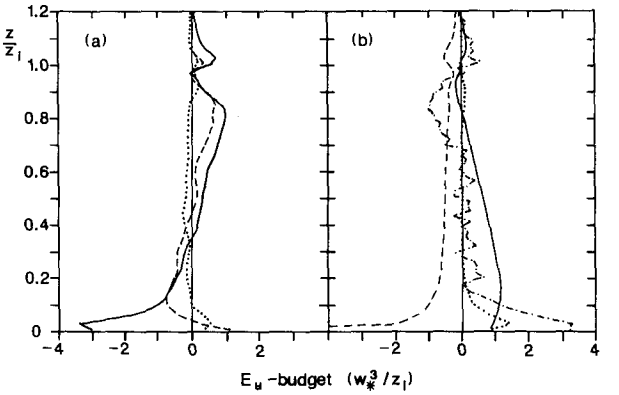

FIG. 7. Contributions to the budget of kinetic energy of turbulent motions in updrafts of the CBL, $\partial E_u/\partial t$ = (a) $-\alpha_u^{-1}\partial(\alpha_u w_u E_u)/\partial z - \alpha_u^{-1}\partial(\alpha_u[w_u''E_u'']_u)/\partial z - [\rho^{-1}\partial(u_i'p')/\partial x_i]_u$ and (b) $[\beta g w'\theta_v']_u - [\epsilon]_u - [u_i'u_j'\partial\bar{u}_i/\partial x_j - u_i'\partial u_i'w'/\partial z]_u - M_{E,u}$. Lines correspond to terms as before except dot-dash line to fourth term in (b).

the full curve in (b), represents the main source of energy. The buoyancy flux in updrafts is larger than its horizontal average, which enters the common ensemble-averaged budget of turbulent kinetic energy (this "total" budget has been shown in Moeng and Wyngaard 1989). The production rate from shear in updrafts [dotted curve in (b)] is smaller than in the total budget because the downstream velocity u in updrafts is smaller than in downdrafts. Anyway, it is important only in the surface layer. Dissipation forms the primary sink term, in particular near the lower surface [dashed in (b)]. In updrafts it is larger than in the total budget because of more vigorous turbulence. An essential source is represented by mixing of turbulent fluid from downdrafts into the updrafts in the lower part of the mixed layer [dash-dotted in (b)]. In the uppermost part ($z > 0.7z_i$), this mixing term contributes to energy loss. Mean updrafts contribute strongly to divergence of advection [full curve in (a)] while small-scale vertical mixing is rather unimportant. Also the work done by pressure fluctuations against velocity fluctuations [dotted curve in (a)] is relatively small throughout the boundary layer. The sum of the first two terms from updrafts and downdrafts (weighted with their respective area fractions) represents the divergence of the "diffusional" transport $-\partial\overline{w'u_i'^2}/2/\partial z$ in the total budget. We find that most of this transport is affected by vertical advection of kinetic energy in updrafts (the downdraft contributions are much smaller and generally of opposite sign).

In the budget for kinetic energy in downdrafts (not plotted), all terms (except for mixing) are of smaller magnitude than those shown for updrafts. Near the bottom of the boundary layer, the divergence of vertical advection forms the most important energy source (whereas it is a sink in updrafts). It is even larger than the buoyancy and shear forcing at this level. The mixing of energy out of updrafts and into downdrafts sums to

zero, see Eq. (18). The mixing provides the main energy source in the upper part of the downdrafts; i.e., downdrafts start to be turbulent not by themselves rather than by turbulence energy gained from updrafts. Such a gain term is necessary to balance the energy sink from negative entrainment heat flux. Hence, we may conjecture that the entrainment is driven mainly by turbulence from updrafts.

c. *Budgets for STBL*

Figures 8 to 11 depict similar budgets for the stratus-topped boundary layer. For this layer, the LES includes the total moisture q as an additional conserved field, and we present a corresponding budget. The heat and moisture budgets are presented in physical units because any definition of convective temperature and moisture scales would be rather arbitrary; they can be defined either in terms of surface, inversion, or layer-integrated fluxes (as given in SM).

The budget of vertical velocity in updrafts, Fig. 8, looks qualitatively similar to that shown in Fig. 4 for the CBL, except for the profile of buoyancy from virtual potential temperature, the full curve in (b). It reflects the additional buoyancy from latent heat release in the cloudy layer and radiative cooling near cloud top. As a consequence, the amplitude of the budget contributions near the inversion are larger in magnitude than in the dry case. They are also larger near the bottom surface because of stronger circulations across the whole boundary layer induced by the additional buoyancy. These circulations have been made visible in the form of composites in Moeng and Schumann (1990). The buoyancy and the fluctuating pressure terms shown in Fig. 8b are balancing each other to a larger degree than in Fig. 4. This would suggest that the STBL updrafts are closer in hydrostatic equilibrium than the CBL updrafts. However, the large nonlinear terms plotted in Fig 8a, which balance each other, show that this flow also is basically nonhydrostatic.

The budget components of vertical velocity in

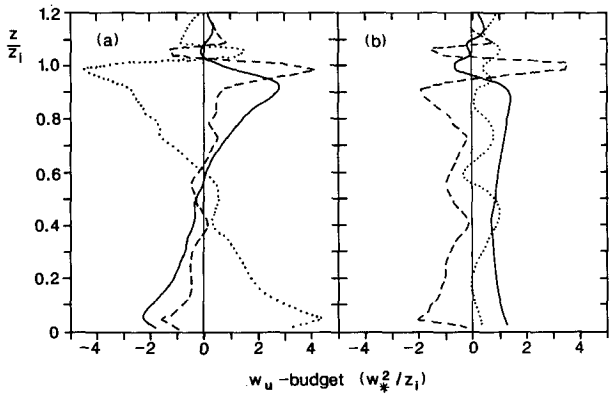

FIG. 8. Same as Fig. 4 for STBL (vertical velocity in updrafts).

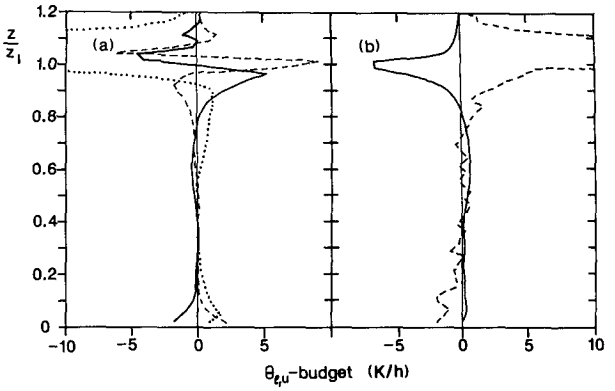

FIG. 9. Contributions to the budget of liquid water potential temperature θ_l in updrafts of the STBL, $\partial\theta_{l,u}/\partial t$ = (a) $-\alpha_u^{-1}\partial(\alpha_u w_u(\theta_u - \bar{\theta}))/\partial z - \alpha_u^{-1}\partial(\alpha_u[w''_u\theta''_u]_u)/\partial z - w_u\,\partial\bar{\theta}/\partial z$ and (b) $[Q_R]_u - M_{\theta,u}$. Line correspondence as in Fig. 5. The dotted cuve in (a) and the dashed curve in (b) reach extreme values of about ± 220 K h^{-1} near the inversion.

downdrafts (not plotted) show about the same profiles as in Fig. 8a and negatively the same as in Fig. 8b. This symmetry is much more pronounced than for the dry case, which is expected since the STBL that we analyze is driven by both the cloud-top radiative cooling and surface heating. Therefore, it is reasonable that updrafts and downdrafts show smaller differences in velocity magnitude and smaller skewness in vertical velocity fluctuations, as discussed in Moeng and Rotunno (1990). In fact, the magnitude of the downward accelerations from mean advection and from the vertical pressure gradient are even a little larger than in the updrafts and this causes the downdrafts to be a little more vigorous than the updrafts.

The budget for horizontal velocity u in x direction in the STBL is not much different from that shown in Fig. 5 for the dry case, except that the amplitudes of the profiles are slightly larger. It is therefore not shown.

Figure 9 exhibits the radiation cooling [full curve in (b)] in a rather thin layer near the cloud top. This cooling enters the budget of the liquid water potential temperature θ_l in this simulation in contrast to the dry case. The cooling in the upper part of the updrafts adds to the production of negative buoyancy, which then drives the downdrafts. In the present case, the cooling is larger than the surface heating (see the source terms in Fig. 9a near the surface), and, therefore, the circulation is driven more by the radiation cooling.

Figure 10 depicts the budget of total moisture in the updrafts of the STBL. The updrafts gain moisture by evaporation from the bottom surface (dashed curve in Fig. 10a). This moisture excess is transported upward by mean vertical motion in the updrafts according to the two advection terms [full and dotted curves in (a)] and increases the moisture at the inversion. This advection is balanced to a large extent by the mixing of relatively dry air from downdrafts into updrafts [full

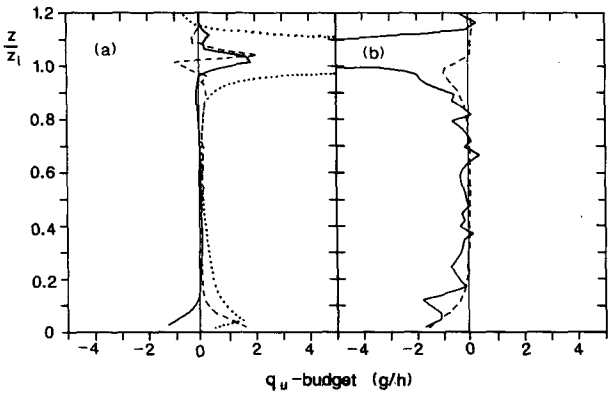

FIG. 10. Contributions to the budget of total moisture (water vapor plus liquid water) in updrafts of the STBL, $\partial q_u/\partial t$ = (a) $-\alpha_u^{-1}\partial(\alpha_u w_u(q_u-\bar{q}))/\partial z - \alpha_u^{-1}\partial(\alpha_u[w_u''q_u'']_u)/\partial z - w_u\partial\bar{q}/\partial z$ and (b) $-M_{q,u}$. Line correspondence as before. The dotted curve in (a) and the full curve in (b) reach extreme values of about ± 8 g h^{-1} near the inversion. The dashed curve in (b) represents the model result, Eq. (25), for the mixing term.

curve in (b)]. In comparison to the mixing near the surface or at the inversion, the net exchange of moisture between updrafts and downdrafts [full curve in (b)] is rather small at intermediate altitudes in the mixed layer, but it is still large in comparison to all other terms of the budget at the same altitude. Since q is a conserved quantity in these simulations, we expect that any passive tracer, emitted at the surface and transported upward, would exhibit the same form of budget.

Finally, Fig. 11 depicts the budget of turbulent kinetic energy in updrafts of the STBL. The results look generally similar to those shown for the CBL in Fig. 7 with a few important differences. The cloud layer induces additional buoyancy fluxes by latent heat release from upward motions of saturated air and by radiation cooling, see full curve in (b). The buoyancy forcing at the cloud levels is much larger than in the dry case. As a consequence, all the transport terms at that level get larger in the STBL than in the CBL. The rather large dissipation [dashed curve in (b)] near the inversion (large in comparison to the mean dissipation of the total budget shown in SM) reflects intensive small-scale turbulence in updrafts at this altitude. The large budget contributions at the surface are induced by strong convective circulations involving the whole layer depth. Again, the lateral mixing forms a very large source term near the surface and the most important sink-term near the inversion. This implies that turbulence is far from local equilibrium (between local general and dissipation) in such updrafts.

Corresponding budgets have been computed also for downdrafts in the STBL (not plotted). The general behavior is as discussed for the CBL, but updrafts and downdrafts are more similar to each other in the STBL than in the CBL. This was noted already for the budget of vertical velocity. Buoyancy forcing in the STBL is of comparable magnitude both in updrafts and downdrafts. Hence, the surface heating, which mainly drives the updrafts, and the cloud-top radiation cooling, which mainly drives the downdrafts, are of comparable importance. The latter is slightly larger and therefore the cloudy downdrafts are more vigorous than the updrafts. The results reveal, as in the dry case, that turbulence in the uppermost part of downdrafts is imported from updrafts, rather than directly driven by buoyancy. This fact should have consequences for entrainment models. It has also been found from composite analysis (Moeng and Schumann 1990) and agrees qualitatively with observations of Nicholls (1989). The results would be different if one changes considerably the ratio between surface heating and cloud-top radiation cooling.

d. Comparison with Chatfield and Brost

Chatfield and Brost (1987) set up a two-stream model of updrafts and downdrafts to describe tracer transport in a CBL. Their concept is similar to ours in that they define the streams in terms of w plumes. By taking the difference between their budget equation for tracers in a plume (their Eq. 7) and our equivalent budget, Eq. (17), we see that they model the mixing term by

$$M_{f,p} = \tfrac{1}{2}(m + |m|)(\bar{f} - f_{1-p}) + \tfrac{1}{2}(m - |m|)(\bar{f} - f_p), \quad m = \frac{\partial}{\partial z}(w_p\alpha_p). \quad (25)$$

Here, the first term is nonzero and the second is zero for the lower part of an updraft where m is positive, and vice versa for the upper part of an updraft where m is negative. For downdrafts just the opposite applies. Thus, an updraft, e.g., increases in f_u at a rate $|m|(f_d - \bar{f})$ in its lower part and decreases at a rate $|m|(f_u - \bar{f})$ in its upper part; this is reasonable. The formula predicts zero mixing in the middle of the boundary layer where the gradient m vanishes.

Chatfield and Brost (1987) determined the param-

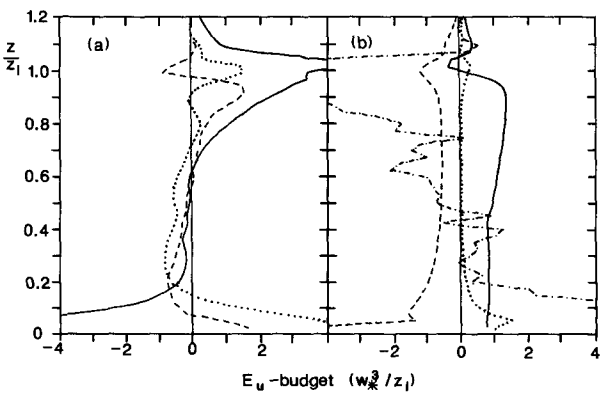

FIG. 11. Same as Fig. 7 for STBL (kinetic energy in updrafts).

eters of the model by fitting the results to dispersion measurements. For example, the plume flux $\alpha_u w_u$, which is an important quantity for such a model, reaches a maximum value of $0.175 w_*$ at about midlevel of the CBL in their model. In view of the database, this is quite close to $0.23 w_*$, which we obtain from the LES (SM).

Figures 6 and 10 contain comparisons between the LES results on the mixing terms $M_{f,u}$ (full curves) and the model predictions from Eq. (25) (dashed curves) for temperature in the CBL and for moisture in the STBL. For this comparison we use the LES results to compute m. We find that the model agrees to first order with the LES, but the LES results generally show larger mixing. Obviously, the model describes only that part of the entrainment which is carried by the mean convective circulation. It does not include the small-scale turbulent mixing which was apparently of minor importance in the applications of Chatfield and Brost (1987). In order to model the small-scale turbulent fluxes, one might add an entrainment model in terms of the plume diameter, an entrainment velocity, and the difference in mean properties between the plumes. For example, Telford (1970) developed such a model where the entrainment velocity is related to the square root of the turbulent kinetic energy within the updrafts.

Our comparison shows that the largest differences appear between the LES results and the modeled mixing near the inversion. Recall that our mixing term includes components of the lateral and the vertical mixing fluxes in the normal direction of the plume's surface (see Fig. 1) whose orientation fluctuates with time. Hence, the LES includes large parts of the vertical mixing across the inversion in this mixing term. On the other hand, Eq. (25) intends to model the lateral mixing only, whereas the vertical mixing was included in Chatfield and Brost (1987) separately by a gradient model that approximates turbulent fluxes within the plumes. In their applications, the fluxes at the inversion were unimportant. Therefore, they could work with eddy diffusivities, which are zero at the inversion. Hence, such models still have to be extended and tested for cases with nonzero entrainment fluxes. As a more formal point we recall that the mixing for w is smaller than for other quantities and, hence, should be modeled differently from that for any other fluctuating quantity in w plumes. But this is irrelevant for Chatfield and Brost (1987), who applied their model only to tracer transport.

e. Comparison with Young

Young (1988) determined the advective parts of the plume budget for vertical velocity. In his analysis of aircraft data it was impossible to separate the mixing term from the effects of pressure forces, which he had to summarize in a residuum. He used a different splitting of the various contributions to the budget and considered:

$$Acceleration + Size + Buoyancy = Residuum,$$

with

$$Acceleration = \frac{\partial}{\partial z}(w_u^2 + [w_u''^2]_u) = \frac{\partial}{\partial z}[w'^2]_u, \quad (26)$$

$$Size = (w_u^2 + [w_u''^2]_u)\alpha_u^{-1}\frac{\partial \alpha_u}{\partial z}$$

$$= [w'^2]_u \alpha_u^{-1}\frac{\partial \alpha_u}{\partial z}, \quad (27)$$

$$Buoyancy = -\beta g[\theta_v']_u. \quad (28)$$

Here, positive quantities represent sink terms of w_u. This form of equation agrees with our derivation if the *Residuum* contains $[-\rho^{-1}\partial p/\partial z]_u - M_{w,u} - \partial w_u/\partial t$. The contributions from the pressure gradient have been plotted in Fig. 4. The largest part of the *Residuum* stems from the gradient of the mean pressure [i.e., from the negative gradient of mean vertical velocity variance, see Eq. (21)], whereas the other parts are relatively small.

In Fig. 12, we compare the LES results for case CBL with the results of Young (1988). We find general agreement, but the measured acceleration magnitude

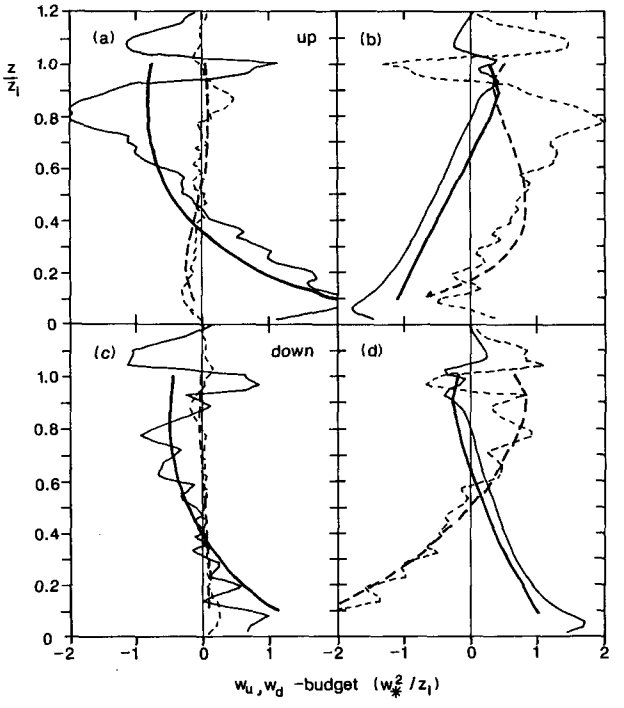

FIG. 12. Comparison with Young (1988), see Eqs. (26) to (28), for the CBL. Upper panels for updrafts, lower panels for downdrafts. Thick curves from Young, thin curves from LES. Left panels: *Acceleration* (full curve) and *size* term (dashed). Right panels: *buoyancy* (full) and *residuum* (dashed).

in updrafts is a little smaller in the upper part of the mixed layer than computed. For downdrafts, the agreement is quite close for all curves. In view of the fact that these profiles are based on vertical derivatives of mean profiles, which exhibit considerable scatter both in the LES and in the measurements, the differences are to be considered small.

4. Conclusions

We have deduced the budget equations for the ensemble of updrafts and downdrafts. The result, Eq. (17), contains a mixing term that defines the source term due to net mixing between the plume under consideration and its environment. This mixing term represents the transport across the surface of a plume at a given height. The surface itself is of complex geometry and moving at its own speed different from the fluid's velocity. By means of Leibniz' rule and the divergence theorem, it is possible to determine the flux across this complicated surface, without knowing the details of this surface, purely from volume integrals, see Eq. (15). Also, we do not need to know explicitly the source terms contributing to the budget.

The method could be applied to any type of plumes in any horizontally homogeneous field. Here we have applied the method to data obtained by the LES-method of Moeng (1984, 1986) for the dry and the stratus-topped convective boundary layer and for w plumes classified according to the sign of the vertical velocity in each individual grid cell.

We have presented budgets for mass or volume, vertical and horizontal momentum, temperature, moisture, and turbulent kinetic energy. Comparable results for w plumes were available only for parts of the budget of vertical velocity from Young (1988) for the CBL. The agreement is satisfactory in this respect. Minor differences have been found in the surface layer and at the inversion where the LES results are affected by resolution limitations.

The results show that in the present case the dry and the cloudy boundary layer are similar in the basic structure of the normalized budget profiles. The latent heat release in cloudy updrafts and the radiational cooling at the top of the stratus layer increase the buoyancy from surface heating. For the given ratio of top cooling and bottom heating, the downdrafts in the STBL are a little stronger than updrafts, but overall the flow and the related budgets of updrafts and downdrafts are more symmetric than in the CBL.

In both cases, the budgets are generally controlled by divergence of vertical advection according to the plume's vertical mean velocity and the vertical mean profiles of the advected fields. However, mixing between updrafts and downdrafts is essential to balance these advections. The net mixing magnitude is small in the middle of the mixed layer, larger in the surface layer, and most important at the inversion, in particular in the cloudy case. Only part of the mixing can be explained with the mean convective circulation. Noncoherent turbulent motions provide the other part. A large portion of the kinetic energy of turbulence in the uppermost part of downdrafts stems from turbulence generated in updrafts. This should be taken into account in modeling entrainment at the inversion. Pressure forces contribute considerably to the exchange of horizontal momentum between updrafts and downdrafts and drive fluid in the upper parts of downdrafts toward the bottom surface. The mixing model by Chatfield and Brost (1987) describes that fraction of the mixing which is induced by the mean convective circulation and the related volume flux. Future work has to consider models that predict the plume's dynamics and account for the small-scale mixing. The results shown in this paper should help in developing such models.

Acknowledgments. We are grateful to G. S. Young, D. A. Randall (who is investigating a similar approach), and the reviewers for useful discussions and comments on an earlier version of this paper. This work was started while the first author was a visiting scientist at the National Center for Atmospheric Research, for which he acknowledges financial support. The National Center for Atmospheric Research is sponsored by the National Science Foundation.

APPENDIX

Source Terms of Various Budgets

The source terms for $f = 1$, $f = \theta_l$, and $f = q$ are simply

$$[Q_1]_p = 0, \quad [Q_\theta]_p = [Q_R]_p, \quad [Q_q]_p = 0, \quad (29)$$

where Q_R is the local heating rate due to radiation. The source term for the x component of the horizontal momentum $u \equiv u_1$ is still quite simple (we neglect the contributions of Coriolis forces and large scale subsidence that are present in the LES simulation but have very small effects in the present case):

$$[Q_u]_p = -\rho^{-1}[\partial p'/\partial x]_p = -\rho^{-1} D_p^{-1}[n_1 e_1 p']_{S_p}, \quad (30)$$

where e_1 is the unit vector in x direction ($x \equiv x_1$) and n_1 the corresponding component of the normal vector. The source term for vertical velocity is composed of a pressure and a buoyancy term:

$$[Q_w]_p = -\rho^{-1}[\partial p'/\partial z]_p - \rho^{-1}\partial \bar{p}/\partial z + [\beta g \theta_v']_p, \quad (31)$$

where $\beta g = g/T$ is the buoyancy coefficient. The term $\bar{p}$ represents the mean pressure induced by turbulence. It does not contain the hydrostatic mean pressure (which does not appear in these equations because we have defined the buoyancy in terms of temperature fluctuations) or any large-scale gradients. As can be seen from the horizontally averaged vertical momen-

tum balance, Eq. (21), the turbulence contribution to the mean pressure equals $\bar{p} = -\rho\overline{w^2}$.

The source term for the plume mean of the kinetic energy of turbulent motions $[E]_p$, $E = u_i'^2/2$, is given by

$$[Q_E]_p = \left[-u_i' u_j' \frac{\partial \overline{u_i}}{\partial x_j} + u_i' \frac{\partial}{\partial z} \overline{u_i' w'} - \frac{\partial}{\partial x_i} (u_i' p'/\rho) - \epsilon + \beta g w' \theta_v' \right]_p . \quad (32)$$

Consistent with the LES, the local stresses are computed from the sum of resolved and SGS stresses. Here, ϵ denotes the local dissipation rate, and this term is evaluated using the SGS model (Moeng 1984). The second term on the right of Eq. (32) is unfamiliar from common models for kinetic energy. It is zero in the horizontal mean but nonzero for averaging over plumes; it is, however, of minor importance in the present convective cases.

REFERENCES

Arakawa, A., and W. H. Schubert, 1974: Interaction of a cumulus cloud ensemble with the large-scale environment, Part I. *J. Atmos. Sci.*, **31**, 674–701.

Betts, A. K., 1973: Non-precipitating cumulus convection and its parameterization. *Quart. J. Roy. Meteor. Soc.*, **99**, 178–196.

Chatfield, R. B., and R. A. Brost, 1987: A two-stream model of the vertical transport of trace species in the convective boundary layer. *J. Geophys. Res.*, **92**(D11), 13 263–13 276.

Hanson, H. P., 1981: On mixing by trade-wind cumuli. *J. Atmos. Sci.*, **38**, 1003–1014.

Lenschow, D. H., and P. L. Stephens 1980: The role of thermals in the convective boundary layer. *Bound.-Layer Meteor.*, **19**, 509–532.

Moeng, C.-H., 1984: A large-eddy-simulation model for the study of planetary boundary-layer turbulence. *J. Atmos. Sci.*, **41**, 2052–2062.

——, 1986: Large-eddy simulation of a stratus-topped boundary layer. Part I: Structure and budgets. *J. Atmos. Sci.*, **43**, 2886–2900.

——, and J. C. Wyngaard, 1989: Evaluation of turbulent transport and dissipation closures in second-order modeling. *J. Atmos. Sci.*, **46**, 2311–2330.

——, and R. Rotunno, 1990: Vertical-velocity skewness in the buoyancy-driven boundary layer. *J. Atmos. Sci.*, **47**, 1149–1162.

——, and U. Schumann, 1990: Composite updraft and downdraft in stratus-topped boundary layer. *Proc. 9th Symposium on Turbulence and Diffusion*, Roskilde, Denmark, Amer. Meteor. Soc., 7–10.

Nicholls, S., 1989: The structure of radiatively driven convection in stratocumulus. *Quart. J. Roy. Meteor. Soc.*, **115**, 487–511.

Penc, R. S., and B. A. Albrecht, 1987: Parametric representation of heat and moisture fluxes in cloud-topped mixed layers. *Bound.-Layer Meteor.*, **38**, 225–248.

Randall, D. A., and G. J. Huffman, 1982: Entrainment and detrainment in a simple cumulus cloud model. *J. Atmos. Sci.*, **39**, 2793–2806.

Rotunno, R., and J. B. Klemp, 1982: The influence of shear-induced pressure gradient on thunderstorm motion. *Mon. Wea. Rev.*, **110**, 136–151.

Schumann, U., and C.-H. Moeng, 1991: Plume fluxes in clear and cloudy convective boundary layers. *J. Atmos. Sci.*, **48**, 1746–1757.

Telford, J. W., 1970: Convective plumes in a convective field. *J. Atmos. Sci.*, **27**, 347–358.

Wang, S., and B. A. Albrecht, 1986: A stratocumulus model with an internal circulation. *J. Atmos. Sci.*, **43**, 2374–2391.

——, and ——, 1990: A mean-gradient model of the dry convective boundary layer. *J. Atmos. Sci.*, **47**, 126–138.

Young, G. S., 1988: Turbulence structure of the convective boundary layer. Part III: The vertical velocity budgets of thermals and their environment. *J. Atmos. Sci.*, **45**, 2039–2049.